Bright Bose-Einstein Gap Solitons of Atoms with Repulsive Interaction

B. Eiermann,[1] Th. Anker,[1] M. Albiez,[1] M. Taglieber,[2] P. Treutlein,[2] K.-P. Marzlin,[3] and M. K. Oberthaler[1]

[1]*Kirchhoff Institut für Physik, Universität Heidelberg, Im Neuenheimer Feld 227, 69120 Heidelberg, Germany*

[2]*Max-Planck-Institut für Quantenoptik und Sektion Physik der Ludwig-Maximilians-Universität, Schellingstrasse 4, 80799 München, Germany*

[3]*Department of Physics and Astronomy, Quantum Information Science Group, University of Calgary, 2500 University Drive NW, Calgary, Alberta, Canada T2N 1N4*

(Received 16 December 2003; published 8 June 2004)

We report on the first experimental observation of bright matter wave solitons for ^{87}Rb atoms with repulsive atom-atom interaction. This counterintuitive situation arises inside a weak periodic potential, where anomalous dispersion can be realized at the Brillouin zone boundary. If the coherent atomic wave packet is prepared at the corresponding band edge, a bright soliton is formed inside the gap. The strength of our system is the precise control of preparation and real time manipulation, allowing the systematic investigation of gap solitons.

DOI: 10.1103/PhysRevLett.92.230401 PACS numbers: 03.75.Be, 03.75.Lm, 05.45.Yv, 05.45.–a

Nonspreading localized wave packets [1]—bright solitons—are a paradigm of nonlinear wave dynamics and are encountered in many different fields, such as physics, biology, oceanography, and telecommunication. Solitons form if the nonlinear dynamics compensates the spreading due to linear dispersion. For atomic matter waves, bright solitons have been demonstrated for which the linear spreading due to vacuum dispersion is compensated by the attractive interaction between atoms [2]. For repulsive atom-atom interaction, dark solitons have also been observed experimentally [3].

In this Letter, we report on the experimental observation of a different type of solitons, which exist only in periodic potentials—bright gap solitons. For weak periodic potentials, the formation of gap solitons has been predicted [4], while discrete solitons [5] should be observable in the case of deep periodic potentials. These phenomena are well known in the field of nonlinear photon optics where the nonlinear propagation properties in periodic refractive index structures have been studied [6]. In our experiments with interacting atoms, a new level of experimental control can be achieved, allowing for the realization of gap solitons for repulsive atom-atom interaction corresponding to a self-defocusing medium. It also opens up the way to study solitons in two- and three-dimensional atomic systems [7].

In our experiment, we investigate the evolution of a Bose-Einstein condensate in a quasi-one-dimensional waveguide with a weak periodic potential superimposed in the direction of the waveguide. In the limit of weak atom-atom interaction, the presence of the periodic potential leads to a modification of the linear propagation; i.e., dispersion [8]. It has been demonstrated that with this system anomalous dispersion can be realized [9], which is the prerequisite for the realization of gap solitons for repulsive atom-atom interaction.

Our experimental observations are shown in Fig. 1 and clearly reveal that after a propagation time of 25 ms a nonspreading wave packet is formed. The observed behavior exhibits the qualitative features of gap soliton formation such as (i) during soliton formation excessive atoms are radiated and spread out over time, (ii) solitons do not change their shape and atom number during propagation, and (iii) gap solitons do not move.

The coherent matter wave packets are generated with ^{87}Rb Bose-Einstein condensates [Fig. 2(a)]. The atoms are initially precooled in a magnetic time-orbiting

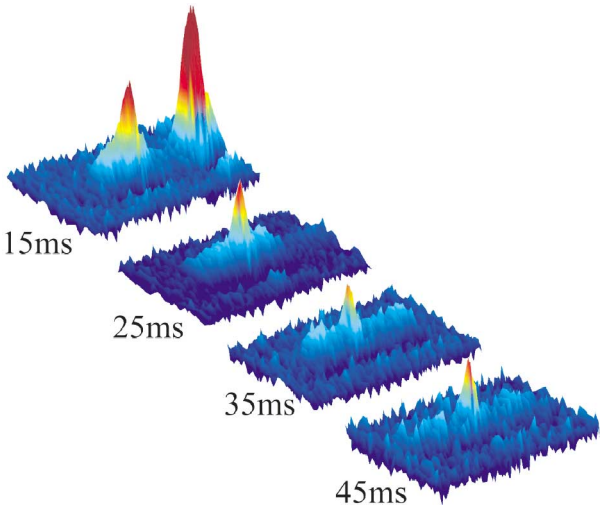

FIG. 1 (color). Observation of bright gap solitons. The atomic density in the negative mass regime deduced from absorption images (430 μm $\times$ 125 μm) averaged over four realizations is shown for different propagation times. After approximately 25 ms, a small peak is formed which does neither change in shape nor in amplitude. Excessive atoms are radiated and disperse over time. After 45 ms only the soliton with $\sim$250 atoms has sufficient density to be clearly observable. The second peak at 15 ms shows the atoms which have been removed by Bragg scattering to generate an initial coherent wave packet consisting of $\sim$900 atoms. For longer observation times, those atoms move out of the imaged region.

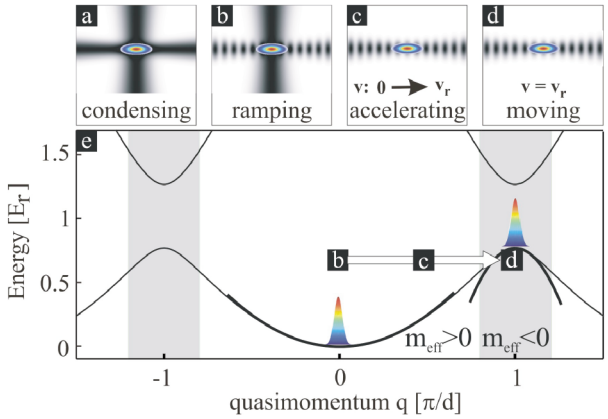

FIG. 2 (color online). Realization of coherent atomic wave packets with negative effective mass utilizing periodic potentials. (a) Top view of the crossed dipole trap geometry used for Bose-Einstein condensation. (b) A periodic potential is ramped up while the atoms are still trapped in the crossed dipole trap realizing the atomic ensemble at $q_c = 0$. (c),(d) The atoms are released into the one-dimensional waveguide and, subsequently, the periodic potential is accelerated to the recoil velocity $v_r = h/\lambda m$. This prepares the atomic wave packet at the band edge of the lowest band. (e) Normal and anomalous (shaded area) dispersion regime in a periodic potential. The single preparation steps are indicated. The shown band structure is calculated for a modulation depth of $V_0 = 1E_r$.

potential trap using the standard technique of forced evaporation leading to a phase space density of ~ 0.03. The atomic ensemble is subsequently adiabatically transferred into a crossed light beam dipole trap ($\lambda =$ 1064 nm, $1/e^2$ waist 60 μm, 500 mW per beam), where further forced evaporation is achieved by lowering the light intensity in the trapping light beams. With this approach, we can generate pure condensates with typically 3×10^4 atoms. By further lowering the light intensity, we can reliably produce coherent wave packets of 3000 atoms. For this atom number no gap solitons have been observed. Therefore, we remove atoms by Bragg scattering [10]. This method splits the condensate coherently leaving an initial wave packet with 900(300) atoms at rest. The periodic potential $V = V_0 \sin^2(\frac{2\pi}{\lambda}x)$ of periodicity $d = \lambda/2$ is realized by a far off-resonant standing light wave of wavelength $\lambda = 783$ nm. The absolute value of the potential depth was calibrated independently by analyzing results on Bragg scattering and Landau-Zener tunneling [11].

After the creation of the coherent wave packet, we ramp-up the periodic potential adiabatically, which prepares the atomic ensemble in the normal dispersion regime at quasimomentum $q = 0$ as indicated in Fig. 2. The dispersion relation for an atom moving in a weak periodic potential exhibits a band structure as a function of quasimomentum q known from the dispersion relation of electrons in crystals [12] [see Fig. 2(e)]. Anomalous dispersion, characterized by a negative effective mass $m_{\text{eff}} < 0$, can be achieved if the mean quasimomentum of the atomic ensemble is shifted to the Brillouin zone boundary corresponding to $q = \pi/d$. This is accomplished by switching off one dipole trap beam, releasing the atomic cloud into the one-dimensional horizontal waveguide [Fig. 2(c)] with transverse and longitudinal trapping frequencies $\omega_\perp = 2\pi \times 85$ Hz, and $w_{||} = 2\pi \times$ 0.5 Hz. Subsequently, the atomic ensemble is prepared at quasimomentum $q = \pi/d$ by accelerating the periodic potential to the recoil velocity $v_r = h/m\lambda$. This is done by introducing an increasing frequency difference between the two laser beams, creating the optical lattice. The acceleration within 1.3 ms is adiabatic; hence, excitations to the upper bands by Landau-Zener transitions are negligible [11]. It is important to note that the strength of the dispersion is under full experimental control. The absolute value of $m_{\text{eff}}(q = \pi/d) = V_0/(V_0 - 8E_r)m$ (weak potential approximation [12]) scales with the modulation depth of the periodic potential, where $E_r = (\hbar^2/2m)(\pi^2/d^2)$ is the recoil energy.

For weak periodic potentials, the full wave function of the condensate is well described by $\Psi(x, t) = A(x, t)u_0^{q_c}(x)\exp(iq_c x)$, where $u_0^{q_c}(x)\exp(iq_c x)$ represents the Bloch state in the lowest band $n = 0$ at the corresponding central quasimomentum q_c. Within the approximation of constant effective mass, the dynamics of the envelope $A(x, t)$ is governed by a one-dimensional nonlinear Schrödinger equation [13]:

$$i\hbar\frac{\partial}{\partial t}A(x, t) = \left(-\frac{\hbar^2}{2m_{\text{eff}}}\frac{\partial^2}{\partial x^2} + g_{1d}|A(x, t)|^2\right)A(x, t),$$

with $g_{1d} = 2\hbar a\omega_\perp\alpha_{nl}$, where α_{nl} is a renormalization factor due to the presence of the periodic potential ($\alpha_{nl} =$ 1.5 for $q = \pi/d$ in the limit of weak periodic potentials [13]), and a is the scattering length. The stationary solution for $q_c = \pi/d$ is given by

$$A(x, t) = \sqrt{N/2x_0}\,\text{sech}(x/x_0)e^{i\hbar t/2m_{\text{eff}}x_0^2},$$

where x_0 is the soliton width and m_{eff} is the effective mass at the band edge. The total number of atoms constituting the soliton is given by

$$N = \frac{\hbar}{\alpha_{nl}\omega_\perp m_{\text{eff}}x_0 a}. \quad (1)$$

This quantitative feature of bright solitons can also be deduced by equating the characteristic energies for dispersion $E_D = \hbar^2/m_{\text{eff}}x_0^2$ and atom-atom interaction $E_{nl} = g_{1d}|A(x = 0, t)|^2$.

A characteristic time scale of solitonic propagation due to the phase evolution can also be identified. In analogy to light optics, the soliton period is given by $T_S = \pi m_{\text{eff}}x_0^2/2\hbar$. Solitonic propagation can be confirmed experimentally if the wave packet does not broaden over time periods much longer than T_S.

Our experimental results in Fig. 1 show the evolution of a gap soliton in the negative mass regime for different

propagation times. The reproducible formation of a single soliton is observed if the initial wave packet is close to the soliton condition, i.e., a well-defined atom number for a given spatial width. The preparation scheme utilizing the Bragg pulse leads to a wave packet containing 900 atoms with a spatial size of $\sim 2.5\ \mu$m (rms). The periodic potential depth was adjusted to $V_0 = 0.70(5)E_r$ leading to $m_{\mathrm{eff}}/m \simeq -0.1$ at the band edge. The soliton can clearly be distinguished from the background after 25 ms, corresponding to three soliton periods. This is consistent with the typical formation time scale of few soliton periods given in nonlinear optics textbooks [14]. After 45 ms of propagation, the density of the radiated atoms drops below the level of detection and thus a pure soliton remains, which has been observed for up to 65 ms. It has been shown that for gap solitons a finite lifetime is expected due to resonant coupling to transversally excited states [15]. In order to understand the background, we numerically integrated the nonpolynomial nonlinear Schrödinger equation [16]. The calculation reveals that the nonquadratic dispersion relation in a periodic potential leads to an initial radiation of atoms. However, the absolute number of atoms in the observed background ($\sim$600 atoms) is higher than the prediction of the employed effective one-dimensional model ($\sim$250 atoms). Therefore we conclude that transverse excitations have to be taken into account to get quantitative agreement. This fact still has to be investigated in more detail.

In the following, we will discuss the experimental facts confirming the successful realization of gap solitons.

In Fig. 3(a), we compare the spreading of wave packets in the normal and anomalous dispersion regime which reveals the expected dramatic difference in wave packet dynamics. The solid circles represent the width of the gap soliton for $m_{\mathrm{eff}}/m = -0.1$, which does not change significantly over time. We deduce a soliton width of $x_0 = 6.0(9)\ \mu$m ($x_{\mathrm{rms}} = 4.5\ \mu$m) from the absorption images where the measured rms width shown in Fig. 3(a) is deconvolved with the optical resolution of $3.8\ \mu$m (rms). In this regime, the wave packet does not spread for more than eight soliton periods [$T_S = 7.7(23)$ ms]. Since our experimental setup allows one to switch from solitonic to dispersive behavior by turning the periodic potential on and off, we can directly compare the solitonic evolution to the expected spreading in the normal dispersion regime. The open circles represent the expansion of a coherent matter wave packet with 300(100) atoms in the normal mass regime $m_{\mathrm{eff}}/m = 1$.

The preparation at the band edge implies that the group velocity of the soliton vanishes. This is confirmed in Fig. 3(b), where the relative position of the soliton with respect to the standing light wave is shown. The maximum group velocity of the lowest band is indicated by the dotted lines. In the experiment, care has to be taken to align the optical dipole trap perpendicular to the gravitational acceleration within 200 μrad. Otherwise

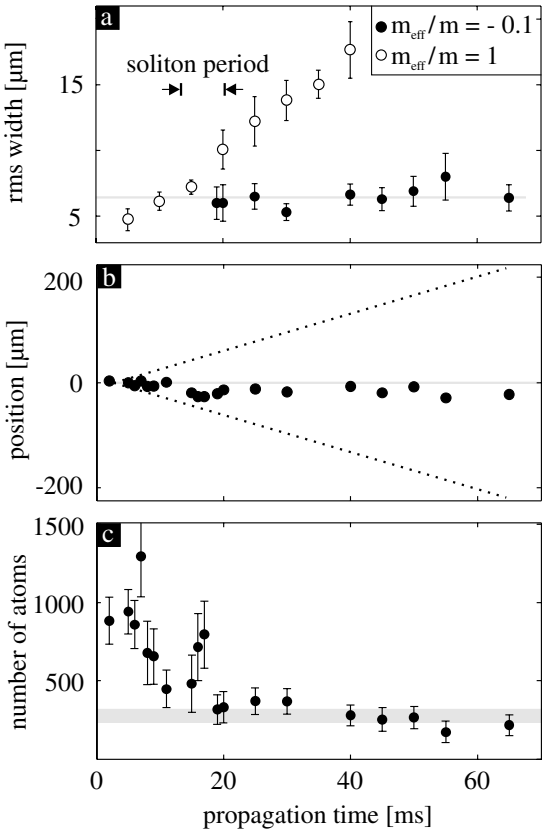

FIG. 3. Characteristic features of the observed gap soliton. (a) Comparison of expansion in the positive and the negative effective mass regime for 300 atoms. While the soliton does not disperse at all over a time of 65 ms, corresponding to more than eight soliton periods (solid circles), a wave packet in the normal mass regime expands significantly (open circles). Each point represents the result of a single realization. The solid line marks the average measured rms width of Gaussian fits to the solitons. Panel (b) shows the position of the soliton in the frame of the periodic potential and reveals that a standing gap soliton has been realized. The dotted lines indicate the positions that correspond to the maximum and the minimum group velocity in the lowest band. (c) Number of atoms in the central peak. The initial atom numbers exhibit large shot to shot fluctuations, which are reduced during the soliton formation. The predicted relation between the number of atoms and the soliton width [Eq. (1)] is indicated by the horizontal bar using the width deduced as shown in (a). Note that this comparison has been done without a free parameter since all contributing parameters are measured independently.

the solitons are accelerated in the direction opposite to the gravitational force revealing their negative mass characteristic.

The calculated number of atoms [Eq. (1)] is indicated by the horizontal bar in Fig. 3(c). The width of the bar represents the expectation within our measurement uncertainties. The observed relation between atom number and width, characteristic for a bright soliton, is in excellent agreement with the simple theoretical prediction without any free parameter.

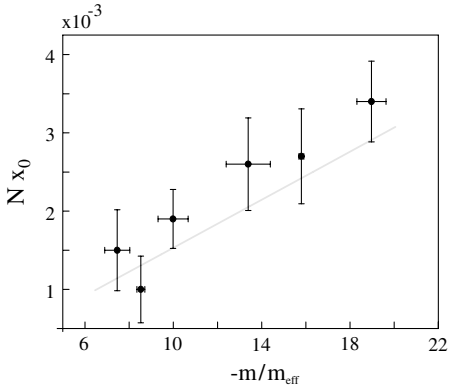

FIG. 4. Scaling properties of a gap soliton. The effective mass was varied experimentally by changing the periodic potential depth. The scaling predicted by Eq. (1) is represented by the solid line and is in good agreement with our experimental observations. The error bars represent the variation of the scaling parameter for different realizations.

As an additional check for soliton formation, we determine the product of atom number and soliton width as a function of the effective mass which is varied by adjusting the modulation depth of the periodic potential. Figure 4 shows the range of effective masses, for which solitons have been observed. For smaller values of $|m_{\mathrm{eff}}|$, corresponding to smaller potential depths, Landau-Zener tunneling does not allow a clean preparation in the negative mass regime, while for larger values the initial number of atoms differs too much from the soliton condition. The observed product of atom number and wave packet width after 40 ms of propagation are shown in Fig. 4 and confirm the behavior expected from Eq. (1). Additionally, our experimental findings reveal that the change of the scaling parameter Nx_0 in Fig. 4 is dominated by the change in the atom number, while the soliton width exhibits only a weak dependence on the effective mass.

The demonstration of gap solitons confirms that Bose condensed atoms combined with a periodic potential allow the precise control of dispersion and nonlinearity. Thus, our setup serves as a versatile new model system for nonlinear wave dynamics. Our experiments show that gap solitons can be created in a reproducible manner. This is an essential prerequisite for the study of soliton collisions. The experiment can be realized by preparing two spatially separated wave packets at the band edge and applying an expulsive potential. Ultimately, atom number squeezed states can be engineered with atomic solitons by implementing schemes analog to those developed for photon number squeezing in light optics [17]. This is interesting from a fundamental point of view and may also have impact on precision atom interferometry experiments.

We wish to thank J. Mlynek for his generous support, and Y. Kivshar, E. Ostrovskaya, A. Sizmann, and B. Brezger for many stimulating discussions. We thank O. Vogelsang and D. Weise for their donation of Ti:sapphire light. This work was supported by the Deutsche Forschungsgemeinschaft, the Emmy Noether Program, and by the European Union, Contract No. HPRN-CT-2000-00125.

[1] J. S. Russell, Report of the 14th Meeting of the British Association for the Advancement of Science, Plates XLVII–LVII (1845), pp. 311–390.
[2] L. Khaykovich *et al.*, Science **296**, 1290 (2002); K. E. Strecker, G. B. Partridge, A. G. Truscott, and R. G. Hulet, Nature (London) **417**, 150 (2002).
[3] S. Burger, K. Bongs, S. Dettmer, W. Ertmer, and K. Sengstock, Phys. Rev. Lett. **83**, 5198 (1999); J. Denschlag *et al.*, Science **287**, 97 (2000).
[4] P. Meystre, *Atom Optics* (Springer-Verlag, New York, 2001), p. 205, and references therein.
[5] A. Trombettoni and A. Smerzi, Phys. Rev. Lett. **86**, 2353 (2001).
[6] B. J. Eggleton, R. E. Slusher, C. M. deSterke, P. A. Krug, and J. E. Sipe, Phys. Rev. Lett. **76**, 1627 (1996); C. M. de Sterke and J. E. Sipe, Prog. Opt. **33**, 203 (1994); D. Neshev, A. A. Sukhorukov, B. Hanna, W. Krolikowski, and Y. Kivshar, nlin.PS/0311059.
[7] H. Saito and M. Ueda, Phys. Rev. Lett. **90**, 040403 (2003); F. Kh. Abdullaev, B. B. Baizakov, and M. Salerno, Phys. Rev. E **68**, 066605 (2003); E. A. Ostrovskaya and Yu. S. Kivshar, Phys. Rev. Lett. **90**, 160407 (2003); V. Ahufinger, A. Sanpera, P. Pedri, L. Santos, and M. Lewenstein, cond-mat/0310042.
[8] S. Burger, F. S. Cataliotti, C. Fort, F. Minardi, M. Inguscio, M. L. Chiofalo, and M. P. Tosi, Phys. Rev. Lett. **86**, 4447 (2001).
[9] B. Eiermann, P. Treutlein, Th. Anker, M. Albiez, M. Taglieber, K.-P. Marzlin, and M. K. Oberthaler, Phys. Rev. Lett. **91**, 060402 (2003).
[10] M. Kozuma, L. Deng, E. W. Hagley, J. Wen, R. Lutwak, K. Helmerson, S. L. Rolston, and W. D. Phillips, Phys. Rev. Lett. **82**, 871 (1999).
[11] B. P. Anderson and M. A. Kasevich, Science **282**, 1686 (1998); O. Morsch, J. Müller, M. Cristiani, D. Ciampini, and E. Arimondo, Phys. Rev. Lett. **87**, 140402 (2001).
[12] N. Ashcroft and N. Mermin, *Solid State Physics* (Saunders, Philadelphia, 1976).
[13] M. Steel and W. Zhang, cond-mat/9810284.
[14] G. P. Agrawal, *Applications of Nonlinear Fiber Optics* (Academic, San Diego, 2001); G. P. Agrawal, *Nonlinear Fiber Optics* (Academic, San Diego, 1995).
[15] K. M. Hilligsøe, M. K. Oberthaler, and K.-P. Marzlin, Phys. Rev. A **66**, 063605 (2002).
[16] L. Salasnich, A. Parola, and L. Reatto, Phys. Rev. A **65**, 043614 (2002).
[17] S. R. Friberg, S. Machida, M. J. Werner, A. Levanon, and T. Mukai, Phys. Rev. Lett. **77**, 3775 (1996).